Crystal structure of oligoacenes under high pressure

M. Oehzelt,* A. Aichholzer, and R. Resel
Institute of Solid State Physics, Graz University of Technology, Petersgasse 16, A-8010 Graz, Austria

G. Heimel
School of Chemistry and Biochemistry, Georgia Institute of Technology, Atlanta, Georgia 30332-0400, USA

E. Venuti and R. G. Della Valle
Dipartimento di Chimica Fisica e Inorganica and INSTM-UdR Bologna, Università di Bologna, Viale Risorgimento 4, I-40136 Bologna, Italy

(Received 20 March 2006; revised manuscript received 17 July 2006; published 5 September 2006)

We report crystal structures of anthracene, tetracene, and pentacene under pressure. Energy dispersive x-ray diffraction experiments up to 9 GPa were performed. Quasiharmonic lattice dynamics calculations are compared to the experimental results and show excellent agreement. The results are discussed with particular emphasis on the pressure dependence of the unit cell dimensions and the rearrangement of the molecules. The high pressure data also allow an analysis of the equation of state of these substances as a function of molecular length. We report the bulk modulus of tetracene and pentacene (B_0=9.0 and 9.6 GPa, respectively) and its pressure derivative (B_0'=7.9 and 6.4, respectively). We find that the unit-cell volume and bulk modulus at ambient pressure follow a linear relationship with the molecular length.

DOI: 10.1103/PhysRevB.74.104103 PACS number(s): 61.50.Ks, 61.10.Nz, 64.30.+t

I. INTRODUCTION

In the last decades π-conjugated molecules have attracted considerable attention, as these systems seem to be promising candidates for low-cost, easy processable materials for electro-optical and electronic applications. Especially the oligoacenes (anthracene, tetracene, pentacene) show high charge carrier mobilities and have been studied extensively for thin film transistor applications.[1–4] While many optical and electronic properties of these compounds can be determined by studying isolated molecules, charge carrier mobilities can only be determined with a detailed knowledge of the packing of the molecules in the solid state.[5]

The packing of the three oligoacenes[6,7] may be described in terms of a layered "herringbone" structure, where the molecules are approximately perpendicular to the plane of the layers. This structure is very similar to that of the oligophenylenes which was the aim of a previous study.[8] There the pressure dependence of the lattice constants is basically the same throughout the series. Based on this structural analogy, that anthracene under pressure behaves like the oligophenylenes,[9] and since also the other oligoacenes exhibit the same layered "herringbone" packing, we were expecting a regular behavior for the lattice parameters as a function of pressure also for tetracene and pentacene, with an analogous compression mechanism. The experiments instead evidence several unexpected anomalies. The quasiharmonic lattice dynamics (QHLD) calculations cast some light on the source of these anomalies, reproducing extremely well both the similarities and the differences among the three oligoacenes.

In this study we report the crystal structure of anthracene, tetracene, and pentacene as a function of pressure. Experimental data obtained from x-ray diffraction measurements up to 9 GPa as well as theoretical results from QHLD calculations[11,12] are presented. From the diffraction data we have determined the lattice constants and then evaluated the bulk modulus and its pressure derivative. The QHLD calculations reproduce the experimentally obtained lattice constants with high precision and allow a detailed analysis of the molecular packing in the solid state.

II. METHODOLOGY

A. Experimental details

The measurements were performed at the beamline F3 at the HASYLAB of the DESY synchrotron facility, Hamburg, Germany. The experiments were conducted in Debye-Scherrer geometry, using white light radiation from a bending magnet.[13] The scattered intensity was recorded with an energy dispersive Ge detector (about 10–60 keV) mounted at a fixed 2θ angle of about 2.5°. After the calibration of the energy scale with the K_{α_1}, K_{α_2} K_{β_1}, and K_{β_2} fluorescence lines of Ag, Eu, Te, Ta, and Se, the detector angle was calibrated with Au and NaCl standards.

Anthracene and tetracene were purchased from Sigma-Aldrich Ltd. and Pentacene from Fluka Ltd. These chemicals are of >99% purity and were therefore used without further processing except grinding in an agate mortar to obtain crystallites with sufficiently small grain sizes.

In order to apply hydrostatic pressure, a Syassen-Holzapfel[14] type diamond anvil cell (DAC) with inconel gaskets was used. A 4:1 methanol:water mixture was employed as pressure transmitting medium. The pressure was determined by the ruby fluorescence method[15] and via the energy position of the 111 and 200 reflections of Au.[16,17] As could be inferred from the linewidth of the ruby fluorescence bands under pressure, hydrostaticity was well maintained. At least two independent pressure runs were conducted for each compound. Typical diffraction patterns for anthracene and pentacene are shown in Fig. 1. The diffraction patterns for tet-

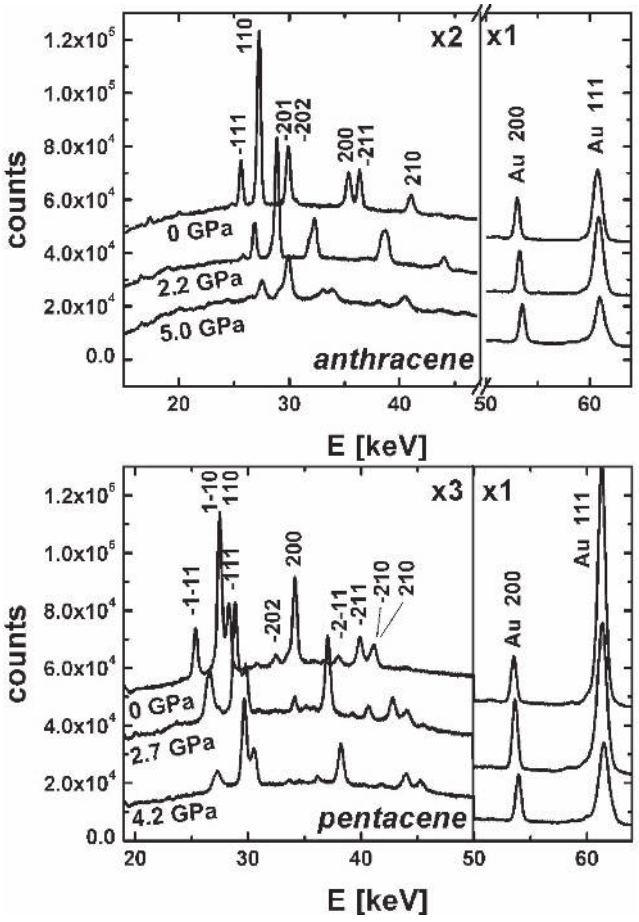

FIG. 1. Selected diffraction pattern of anthracene and pentacene at various pressures. Strong diffraction peaks are labeled by their Miller indices. At higher energies two gold peaks are shown which are used to determine the pressure. The count rate at the lower energy range is multiplied by two for anthracene and three for pentacene, respectively.

racene are very similar to pentacene and therefore not shown. The low energy region is multiplied by two for anthracene and three for pentacene to make the organic peaks more visible compared to the gold peaks shown at the high energy region of the diffraction pattern. The most intense peaks are indexed and clearly a shift of the diffraction peak toward higher energy can be seen.

B. Refinement

The Bragg peaks in the energy dispersive x-ray diffraction (EDXD) patterns are rather broad because of the low energy resolution. Due to the resulting strong overlap between adjacent reflections and the limited number of observed peaks ($\leqslant 20$), we could not perform a Rietveld refinement on the data, which would have allowed us to extract additional structural information concerning the atomic positions within the unit cell. Instead, a LeBail fit[18] was performed on the experimental diffraction patterns to determine the unit cell parameters as a function of pressure. The refinement of the structural parameters was done with GSAS.[19] The peaks were fitted with pseudo Voight functions. The patterns at ambient conditions were refined using starting parameters of the known single crystal structures.[6,7,20] The parameters obtained in the refinement at one pressure point were taken as input for the next higher pressure point. This procedure guarantees good starting fit parameters at all pressures.

C. Theoretical calculations

Following a well-tested procedure for calculating crystal structures as a function of pressure and temperature,[21,22] we start from the *ab initio* geometry and atomic charges of the isolated molecules of anthracene, tetracene, and pentacene. These data were determined with the GAUSSIAN98 program[23] (revision A.5) using the 6-31G(d) basis set combined with the B3LYP exchange correlation functional.[23,24] The *ab initio* geometry is employed to model the crystal structure, using the experimental[6,7] molecular arrangement to build the initial lattice structure. The interactions are given by an intermolecular potential Φ described by an atom-atom Buckingham model,[25] with Williams parameter set IV,[26] combined with an electrostatic contribution represented by a set of *ab initio* atomic charges. Instead of the Mulliken charges, we prefer the "ESP" potential derived charges, which describe directly the electrostatic potential.[23] The convergence of the electrostatic interactions is accelerated with Ewald's method.[25]

The effects of temperature T and pressure p are taken into account by calculating the structures of minimum Gibbs energy $G(p,T)$ with quasiharmonic lattice dynamics[11,12] (QHLD) methods. In this method, where the vibrational Gibbs energy of the phonons is estimated in the harmonic approximation, the Gibbs energy of the system is $G(p,T) = \Phi + pV + \Sigma_i h\nu_i/2 + k_B T \Sigma_i \ln[1-\exp(-h\nu_i/k_B T)]$. Here V is the molar volume, $\Sigma_i h\nu_i/2$ is the zero-point energy, and the last term is the entropic contribution. The sums are extended to all phonon frequencies ν_i. Given the initial lattice structure, one computes Φ and its second derivatives with respect to the displacements of the molecular coordinates. The second derivatives form the dynamical matrix, which is numerically diagonalized to obtain the phonon frequencies ν_i. The structure as a function of p and T is then determined self-consistently by minimizing $G(p,T)$ with respect to lattice parameters, molecular positions, and orientations.

To simplify the discussion we only present results in which all molecules are maintained as rigid units, neglecting the effects of the intramolecular degrees of freedom. This choice is justified by the observation that for the three acenes, as already noticed for other compounds,[10,21] these effects decrease rapidly at high pressure, where they are overwhelmed by the pV term. In preliminary calculations, in fact, we actually allowed for the coupling between lattice and intramolecular vibrations, using an excitonlike model described elsewhere.[21,22,25] Even for pentacene, the most flexible of the three acenes, the volume differences due to the intramolecular vibrations are quite negligible, ranging from 1.4% (at ambient conditions) to 0.4% (at 10 GPa).

The accuracy of the calculations of course depends on the potential model, which in this case was fitted to lattice structure, compressibility, lattice frequencies, and sublimation energy of many different hydrocarbon compounds.[26] Due to its

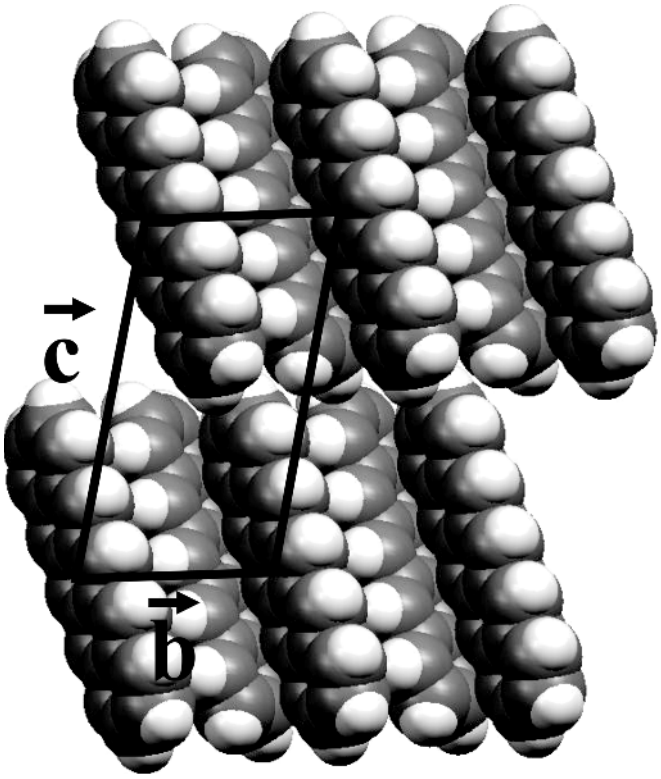

FIG. 2. Two herringbone layers of pentacene are shown in a projection onto the *bc* plane of the unit cell.

origin, the potential effectively accounts for the solid state average of van der Waals interactions, induction effects, and other many body forces. With this potential model, in previous QHLD calculations on the acenes, we have reproduced extremely well the experimental crystal structures of benzene[11] and naphthalene[10] as a function of T or p, and the x-ray structures of all completely known polymorphs of tetracene[27] and pentacene[28] at ambient pressure. Typical differences between calculations and experiments are about 3% for the unit cell axes and angles and 1% for the volume. On the basis of our past experience, we expect to obtain results of comparable quality for the three longer acenes under pressure.

D. Characteristic distances and angles

At ambient conditions anthracene[29] crystallizes in the monoclinic space group $P2_1/a$, while tetracene and pentacene crystallize[30,31] in the triclinic space group $P\bar{1}$. Despite this difference, the arrangement of the molecules within the unit cell is very similar for these oligoacenes. There are always two translationally inequivalent molecules per unit cell ($Z=2$) at positions 000 and $\frac{1}{2}\frac{1}{2}0$. The molecules sit on layers parallel to the *ab* plane, with the long molecular axis approximately perpendicular to the plane of the layer. Neighboring molecules within a layer are twisted with respect to each other, forming a "herringbone pattern." Figure 2 shows a projection onto the *bc* plane of pentacene, presenting two such layers and the arrangement of the molecules within the layers.

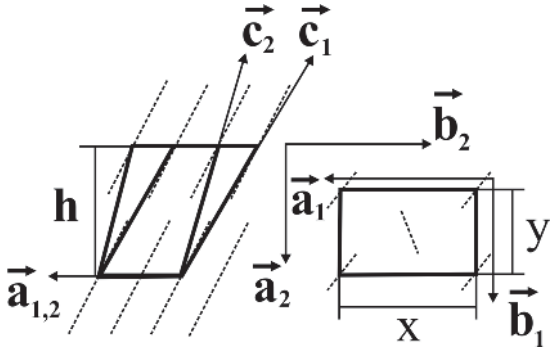

FIG. 3. Cell conventions for the oligoacenes as used in literature (Refs. 29–31). The index 1 indicates the convention for anthracene, 2 that for tetracene and pentacene. The characteristic distances used in this paper are the layer thickness h, and the long and the short herringbone distances x and y.

The comparison between the various oligoacene structures is not straightforward, as different crystallographic conventions hold for triclinic and monoclinic lattices. These conventions lead to lattice constants in the order $a<b<c$ for tetracene and pentacene, and $b<a<c$ for anthracene. To compare the three oligoacenes independently of the different conventional cells adopted in the literature,[29–31] we have chosen a set of characteristic intermolecular distances and angles describing the molecular arrangement within the herringbone structure.[8]

The characteristic distances, named h, x, and y, are illustrated in Fig. 3, together with their relationships to the cell parameters used in the literature. The distance h can be described as the layer thickness (see Fig. 3, left panel). This quantity is in fact d_{001} for all investigated crystal structures (since the longest lattice constant is always c). The two remaining parameters x and y describe the distances in the *ab* plane. The typical herringbone arrangement within the plane, where the molecules are twisted with respect to each other, is shown in Fig. 3 (right panel). In this structure it is always possible to identify a long and a short distance, which we denote as x and y, respectively. For anthracene x and y correspond to the lattice constants a and b. This correspondence is reversed for tetracene and pentacene.

In addition to the characteristic distances, we define the angles θ, δ, and χ, describing the relative orientation of the molecules within the herringbone structure and the setting with respect to the lattice. The three angles are illustrated in Fig. 4 and are defined as follows: θ (herringbone angle) is the angle between the planes of two inequivalent molecules; δ (tilting angle) is the angle between the long molecular axes of two inequivalent molecules; χ (setting angle) is the angle between the long molecular axis of one molecule and the vector c^* normal to the *ab* plane. Due to symmetry reasons, for tetracene and pentacene (space group $P\bar{1}$) the two translationally inequivalent molecules can have different setting angles χ_1 and χ_2, whereas for anthracene (space group $P2_1/a$) all molecules have the same setting χ.

III. RESULTS AND DISCUSSION

The immediate results of this work are the measured and computed lattice parameters (a, b, c, α, β, and γ) as a func-

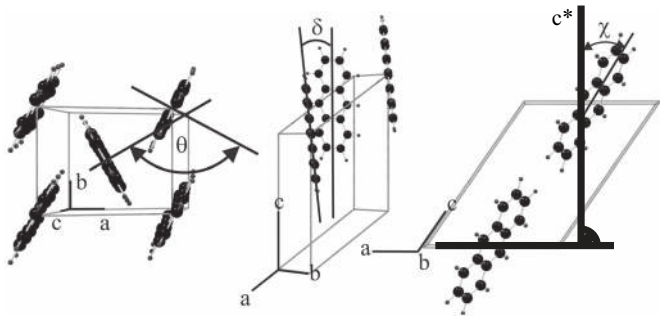

FIG. 4. The three orientation angles of the molecules as they are used within this paper, illustrated for anthracene.

tion of pressure. Such data are part of the supplementary material accessible via the Internet[32] and also available from the authors upon request. Previous measurements for anthracene have been published elsewhere.[9] The measured and computed lattice parameters at ambient conditions are reported in Table I. Here we notice that the measured lattice parameters at ambient conditions are found to be in near perfect agreement with the literature data[6,7,20] and that the computed parameters are good.

As previously discussed, in this paper we focus on characteristic distances and angles, chosen to provide a description independent of the different conventions adopted in the literature. The experimental and theoretical characteristic distances, which are closely correlated to the unit cell dimensions, are shown in Fig. 5. Experimental and theoretical data (represented in the figure as closed and open symbols, respectively) are in very good agreement for all acenes at all pressures. The long distance x decreases with pressure almost twice as much as the short distance y. In fact, the compression in the x direction is around 1.1 Å and the compression in the y direction is around 0.5 Å up to 9 GPa. This

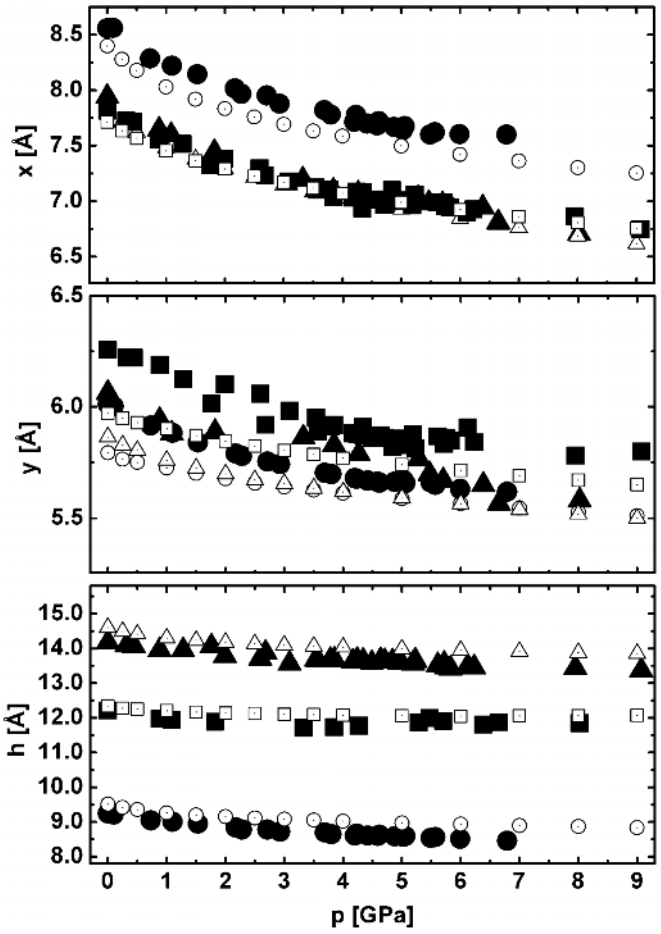

FIG. 5. Unit cell dimensions as a function of pressure for the oligoacenes. Data for anthracene, tetracene, and pentacene, are represented by circles, squares, and triangles, respectively. Closed symbols represent experiments; open symbols represent calculations.

TABLE I. Experimental and computed lattice parameters a, b, c, α, β, and γ for anthracene, tetracene, and pentacene at ambient conditions. The unit cell volume V_0 at ambient conditions, the bulk modulus B_0, and its pressure derivative B_0', obtained by fitting the Murnaghan EOS to the experimental and calculated data are also given, along with the reduced least-squares sum χ^2 of the fit.

	Anthracene		Tetracene		Pentacene	
	Expt.	Calc.	Expt.	Calc.	Expt.	Calc.
a [Å]	8.557	8.399	6.064	5.865	6.256	5.971
b [Å]	6.012	5.793	7.943	7.810	7.813	7.714
c [Å]	11.186	11.199	12.65	12.770	14.615	14.911
α [°]	90	90	101.31	101.71	76.11	79.04
β [°]	124.24	121.87	99.04	98.21	86.85	85.22
γ [°]	90	90	94.15	93.38	84.79	85.59
V_0 [Å^3]	477.3±1.6	462.7	584.7±5.7	564.5	696.0±3.7	670.6
B_0 [GPa]	8.4±0.6	8.5±0.1	9.0±2.0	10.3±0.2	9.6±1.0	11.2±0.1
B_0'	6.3±0.4	8.7±0.1	7.9±1.2	8.5±0.1	6.4±0.5	8.6±0.1
χ^2 [Å^6]	4.5	0.5	34.1	0.6	23.5	0.6

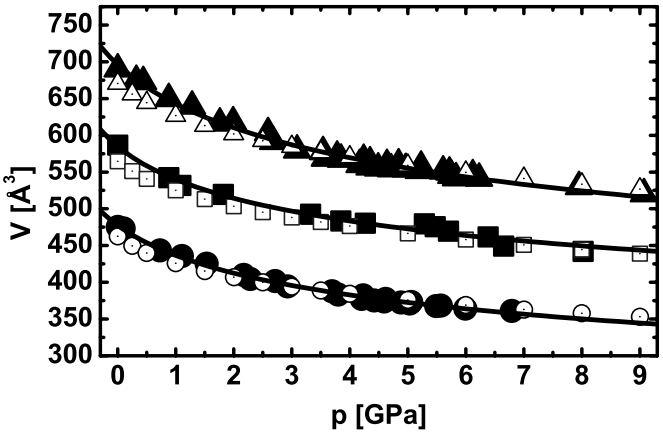

FIG. 6. Volume for the oligoacenes as a function of pressure. The curves are fits to the experimental data with the Murnaghan equation of state. A very good fit between the Murnaghan EOS and the experimental as well as for the theoretical data is obtained. The extracted values for the bulk modulus and its pressure derivative are summerized in Table I. Symbols are as in Fig. 5.

behavior seems to be characteristic for small molecules in the herringbone arrangement as it has also been observed for the oligophenylenes.[8] The values of y are essentially the same for the three substances, while the values for x are similar for pentacene and tetracene, but show an offset for anthracene. Nevertheless, the pressure dependence is analogous in all cases. The layer thickness h follows an anomalous behavior with pressure. By analogy with the case of the oligophenylenes,[8] one would expect three equally spaced curves with the same curvature, since the packing of the oligoacenes is very similar (see Fig. 5). At ambient conditions the gap between anthracene and tetracene is considerably bigger than the gap between tetracene and pentacene. The pressure dependency of the layer thickness for tetracene is also different from that of the other acenes. In contrast, the pressure dependency of the unit cell volumes depicted in Fig. 6 does not show this anomaly anymore. Here the curves are approximately equally spaced and also the curvatures are comparable. To explain this behavior we have to analyze in detail the rearrangement of the molecules under pressure.

The characteristic angles as a function of pressure are shown in Fig. 7. Experimental angles under pressure are not available, because no data on the atomic coordinates could be obtained in the diffraction measurements. The experimental angles at ambient pressure have been deduced from the published crystallographic coordinates.[6,7,20] Since experimental and computed angles are in good agreement at ambient conditions, and since the match between the calculated pressure dependence of the crystal structure and the experimental lattice parameter is excellent, we consider the calculated crystal structures as a reliable source of information on the molecular orientations under pressure.

For the angles, like for the distances, the behavior of the three oligoacenes is very similar when looking at the changes in the herringbone structure. The herringbone angle θ has the same behavior for anthracene, tetracene, and pentacene. In fact, θ increases when applying pressure, which is expected, as the distance x decreases two times the amount of y. This

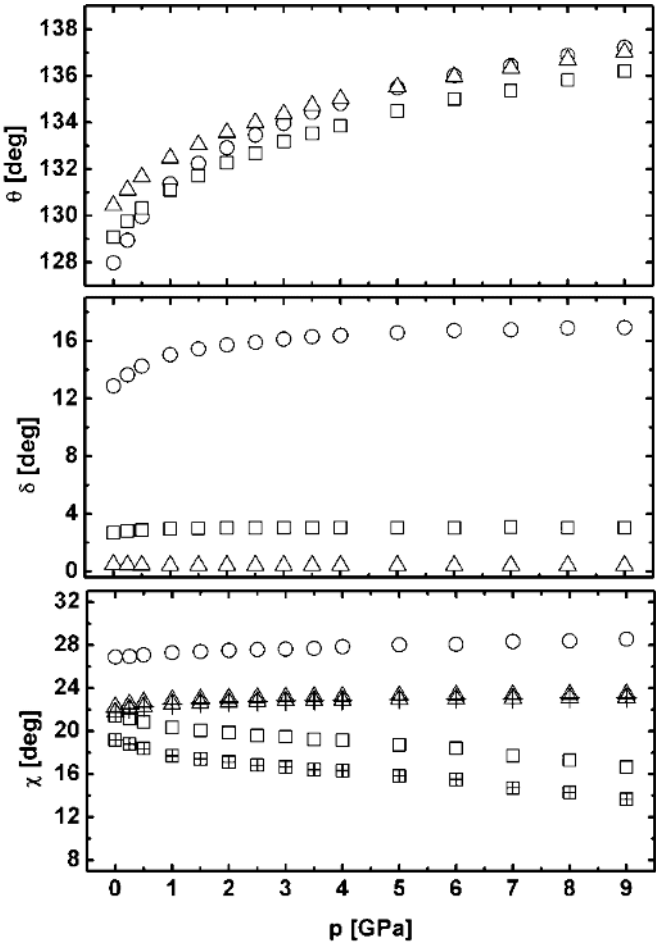

FIG. 7. Characteristic angles for the oligoacenes as a function of pressure. The χ angles for tetracene and pentacene molecules at 000 and $\frac{1}{2}\frac{1}{2}0$ positions are represented by open and crossed symbols, respectively. For anthracene the two molecules have the same χ angle. Symbols are as in Fig. 5.

change in x and y can be easily induced by rotating the molecules toward a more parallel orientation (see also Fig. 4), which increases the angle θ.

The tilting angle δ between the long molecular axis of two neighboring molecules is also shown in Fig. 7. This angle increases with pressure from 13° to about 17° for anthracene, which presents the highest value for the oligoacene series. For tetracene it increases negligibly from 2.6° to 3°, while for pentacene it is approximately constant at 0.5° over the investigated pressure range. It can be noticed that the angle δ decreases as the molecular length increases. This behavior is easily understood because increasing the ratio between the length and the breadth of the molecules favors a more parallel arrangement, leading to a denser molecular packing.[9]

The behavior of the setting angle χ is more complex. For tetracene the two inequivalent molecules in the unit cell have angles χ_1 and χ_2 which differ by $\Delta\chi \approx 3°$. This difference is much smaller for pentacene, for which $\Delta\chi \approx 0.5°$. For anthracene, as already mentioned, the two molecules in the unit cell are connected by symmetry and have exactly identical χ angles. Beside this, there are important differences in the

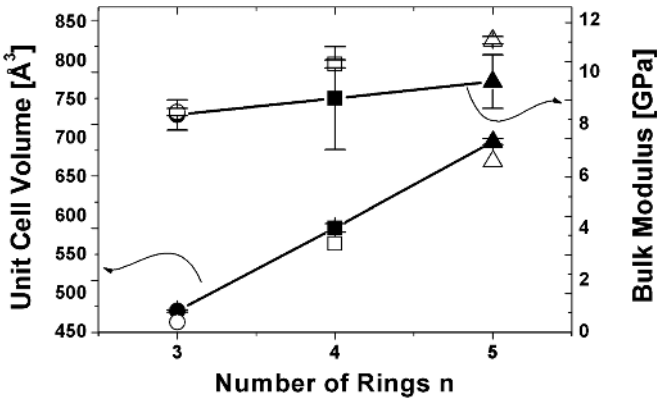

FIG. 8. The unit cell volume at ambient conditions and the bulk modulus show a linear relationship with the number n of phenyl rings in the molecule (3 for anthracene, 4 for tetracene, and 5 for pentacene). Symbols are as in Fig. 5.

behavior under compression. As for the oligophenylenes,[8] and as expected, the angle χ increases with pressure for anthracene and pentacene, which means that the layer thickness h is reduced (see also Fig. 5). For tetracene the pressure dependence shows the reverse trend. It means that the molecules tend to become perpendicular to the layers. While this behavior is not expected, it can explain the differences in the pressure dependence of the layer thickness h, where tetracene shows a different trend compared to anthracene and pentacene.

As shown in Fig. 6, we have computed the unit cell volume as a function of pressure from the experimental data. Starting from these results we have fitted an equation of state (EOS) to the data and obtained the bulk modulus. As shown in previous works[8,9] the Murnaghan EOS[33] is very suitable to describe the compressibility of molecular crystals. The analytical form of the Murnaghan EOS we have used is

$$V = V_0\left(1 + \frac{B_0' p}{B_0}\right)^{-1/B_0'}, \tag{1}$$

where B_0 is the bulk modulus and B_0' is its derivative with pressure. In Fig. 6 the unit cell volumes are plotted as a function of pressure together with the best fits according to Eq. (1) for the experimental datasets. The fit results are given in Table I. The parameters B_0 and B_0' for anthracene are in agreement with the literature values.[9] The parameters for tetracene and pentacene had not been reported before. In Fig. 8 the volume of the unit cell at ambient conditions and the bulk modulus are plotted against the number n of phenyl rings in the individual molecules. As for the oligophenylenes, we notice a good linear relationship of both V_0 and B_0 as a function of n.

IV. CONCLUSION

In this study the crystal structure of three different molecular crystals under pressure is investigated experimentally and theoretically. Experiments up to 9 GPa as well as theoretical calculations using QHLD methods were performed and very good agreement between the experiments and the calculations was found. Our experimental data also match the previous measurements on anthracene[34] and tetracene[35] (up to 2.77 and 0.35 GPa, respectively). No evidence of phase transitions was detected in the investigated pressure range. In particular, we have not identified the high pressure phase known to exist for tetracene.[27,36] In practice, this was to be expected, since the two phases of tetracene[31,36] are quite similar and the resolution of our energy dispersive x-ray diffraction method is small in comparison to angle dispersive methods.

While a series consisting of only three molecules is certainly insufficient to establish a universal relationship, it is nevertheless surprising to observe linear dependencies with molecular size, especially as the details of the packing under pressure show large differences. A linear relationship has been found for the unit cell volume and the bulk modulus as a function of molecular size. This trend is surprising because the three oligoacenes have different crystal symmetries, with anthracene having a monoclinic unit cell and tetracene and pentacene having a triclinic unit cell, and is even more interesting as the rearrangements of the molecules under pressure show different behaviors. For anthracene and pentacene the herringbone layer thickness tends to decrease with pressure, while for tetracene the layer thickness remains practically constant. All three molecules show similar increasing trends of the herringbone angle with pressure, leading to a more cofacial arrangement of the molecules within the herringbone layers.

The QHLD calculations clearly capture the essential physics of these systems, since they describe extremely well the experimental data, reproducing both the similarities and the differences among the three oligoacenes. By comparing experimental and theoretical information, we have obtained an internally consistent, and highly plausible, description of the subtle interplay between the changes in the intermolecular distances and angles which take place under compression. However, we have been unable to identify the precise origin of the different behavior under pressure, which remains unknown and requires further investigations.

ACKNOWLEDGMENTS

We would like to thank Felix Porsch for the help with the beamline instrumentation and x-ray measurements. We acknowledge the financial support by the DESY-FSB project I-00-005EC. G.H. gratefully acknowledges the financial support of the Austrian Science Foundation FWF (Erwin-Schrödinger Grant No. J2419-N02).

*Electronic address: martin.oehzelt@tugraz.at

[1] N. Karl, *Organic Semiconductors*, edited by O. Madelung, Landolt-Börnstein, New Series, Group III, Vol. 17, Pt. A (Springer-Verlag, Berlin, 1985).
[2] C. D. Dimitrakopoulos, A. R. Brown, and A. Pomp, J. Appl. Phys. **80**, 2501 (1996).
[3] J.-J. Lin, D. J. Gundlach, S. Nelson, and T. N. Jackson, IEEE Electron Device Lett. **18**, 606 (1997).
[4] G. Horowitz, Adv. Mater. (Weinheim, Ger.) **10**, 365 (1998).
[5] V. C. Sundar, J. Zaumseil, V. Podzorov, E. Menard, R. L. Willett, T. Someya, M. E. Gershenson, and J. A. Rogers, Science **303**, 1644 (2004).
[6] D. W. J. Cruickshank, Acta Crystallogr. **9**, 915 (1956).
[7] D. Holmes, S. Kumaraswamy, A. J. Matzger, and K. P. Vollhardt, Chem.-Eur. J. **5**, 3399 (1999).
[8] G. Heimel, P. Puschnig, M. Oehzelt, K. Hummer, B. Koppelhuber-Bitschnau, F. Porsch, C. Ambrosch-Draxl, and R. Resel, J. Phys.: Condens. Matter **15**, 3375 (2003).
[9] M. Oehzelt, G. Heimel, R. Resel, P. Puschnig, K. Hummer, C. Ambrosch-Draxl, K. Takemura, and A. Nakayama, J. Chem. Phys. **119**, 1078 (2003).
[10] R. G. Della Valle, E. Venuti, and A. Brillante, Chem. Phys. **198**, 79 (1995).
[11] R. G. Della Valle, E. Venuti, and A. Brillante, Chem. Phys. **202**, 231 (1996).
[12] R. G. Della Valle and E. Venuti, Phys. Rev. B **58**, 206 (1998).
[13] J. W. Otto, Nucl. Instrum. Methods Phys. Res. A **384**, 552 (1997).
[14] A. Jayaraman, Rev. Mod. Phys. **55**, 65 (1983).
[15] H. K. Mao. J. Xu, and P. M. Bell, J. Geophys. Res. **91** (B5), 4673 (1986).
[16] D. L. Heinz and R. Jeanloz, J. Appl. Phys. **55**, 885 (1984).
[17] O. L. Anderson, D. G. Isaak, and S. Yamamoto, J. Appl. Phys. **65**, 1534 (1988).
[18] A. LeBail and D. Louer, Bull. Soc. Fr. Mineral. Cristallogr. **99**, 211 (1976).
[19] R. B. Von Dreele and A. C. Larson (unpublished).
[20] C. C. Mattheus, A. B. Dros, J. Baas, A. Meetsma, J. L. de Boer, and T. T. M. Palstra, Acta Crystallogr., Sect. C: Cryst. Struct. Commun. **57**, 939 (2001).
[21] R. G. Della Valle, E. Venuti, L. Farina, and A. Brillante, Chem. Phys. **273**, 197 (2001).
[22] A. Girlando, M. Masino, G. Visentini, R. G. Della Valle, A. Brillante, and E. Venuti, Phys. Rev. B **62**, 14476 (2000).
[23] M. J. Frisch *et al.*, GAUSSIAN98, Revision A.5 (Gaussian, Inc., Pittsburgh, PA, 1998).
[24] C. Lee, W. Yang, and R. G. Parr, Phys. Rev. B **37**, 785 (1988).
[25] S. Califano, V. Schettino, and N. Neto, *Lattice Dynamics of Molecular Crystals* (Springer-Verlag, Berlin, 1981).
[26] D. E. Williams, J. Chem. Phys. **47**, 4680 (1967).
[27] E. Venuti, R. G. Della Valle, L. Farina, A. Brillante, M. Masino, and A. Girlando, Phys. Rev. B **70**, 104106 (2004).
[28] R. G. Della Valle, E. Venuti, L. Farina, A. Brillante, M. Masino, and A. Girlando, J. Phys. Chem. B **108**, 1822 (2004).
[29] R. Mason, Acta Crystallogr. **17**, 547 (1964).
[30] R. B. Campbell, J. M. Robertson, and J. Trotter, Acta Crystallogr. **14**, 705 (1961).
[31] R. B. Campbell, J. M. Roberston, and J. Trotter, Acta Crystallogr. **15**, 289 (1962).
[32] See EPAPS Document No. E-PRBMDO-74-028634 for a complete set of lattice constants as a function of pressure as obtained from the experiment as well as from the theoretical calculations. In addition, a table with all calculated angles is supplied. This document can be reached via a direct link in the online article's HTML reference section or via the EPAPS homepage (http://www.aip.org/pubservs/epaps.html).
[33] F. D. Murnaghan, Proc. Natl. Acad. Sci. U.S.A. **30**, 244 (1944).
[34] J. M. Leger and H. Aloualiti, Solid State Commun. **79**, 901 (1991).
[35] A. M. Pivovar, J. E. Curtis, J. B. Leao, R. J. Chesterfield, and C. D. Frisbie, Chem. Phys. **325**, 138 (2006).
[36] U. Sondermann, A. Kutoglu, and H. Bässler, J. Phys. Chem. **89**, 1735 (1985).